Electron Transfer Rates in Bridged Molecular Systems 2. A Steady-State Analysis of Coherent Tunneling and Thermal Transitions†

Dvira Segal and Abraham Nitzan*

School of Chemistry, The Sackler Faculty of Science, Tel Aviv University, Tel Aviv, 69978 Israel

William B. Davis,‡ Michael R. Wasielewski,‡,§ and Mark A. Ratner‡

Department of Chemistry, Northwestern University, 2145 North Sheridan Road, Evanston, Illinois 60208-3113, and Chemistry Division, Argonne National Laboratory, Argonne, Illinois 60439-4831

Received: September 14, 1999

The effect of dephasing and relaxation on electron transfer in bridged molecular systems is investigated using a simple molecular model. The interaction between the molecular system and the thermal environment is described on the level of the Redfield theory, modified when needed for the description of steady-state situations. Noting that transient as well as steady-state measurements are possible in such system, we discuss the relationship between the rates obtained from these different types of experiments and, in particular, the conditions under which these rates are the same. Also, a formal relation between the *steady-state rate* for electron transfer across a molecular bridge and the *conductance* of this bridge when placed between two metal contacts is established. The effect of dephasing and relaxation on the electron transfer is investigated, and new observations are made with regard to the transition from the superexchange to the thermal (hopping through bridge) regime of the transfer process. In particular, the rate is temperature-independent in the superexchange regime, and its dependence on the bridge length (N) is exponential, $\exp(-\beta N)$. The rate behaves like $(\alpha_1 + \alpha_2 N)^{-1} \exp(-\Delta E/k_B T)$ beyond a crossover value of N, where ΔE is the energy gap between the donor/acceptor and the bridge levels, and where α_1 and α_2 are characteristic times for activation onto the bridge and diffusion in the bridge, respectively. We find that, in typical cases, $\alpha_1 \gg \alpha_2$, and therefore, a region of very weak N dependence is expected before the Ohmic behavior, N^{-1}, is established for large enough N. In addition, a relatively weak exponential dependence, $\exp(-\alpha N)$, is expected for long bridges if competing processes capture electrons away from the bridge sites. Finally, we consider ways to distinguish experimentally between the thermal and the tunneling routes.

1. Introduction

Coupling to solvent is a major factor in electron-transfer (ET) reactions. Standard theory[1,2] invokes solvent nuclear motion as a necessary prerequisite for creating configurations in which electron transfer can take place without violating energy conservation. The coupling of the ET reactant and product to other *electronic* states often dominates the electronic coupling between the donor and acceptor species. This is most clearly exemplified by long-range electron transfer in bridged molecular systems.[3−6] For example, in going from a saturated organic bridge to an unsaturated one, the rates of ET from a porphyrin donor to a quinone acceptor can increase by several orders of magnitude, even though the donor−acceptor distance, driving force, and relative geometry do not vary much in the two donor−bridge−acceptor (DBA) ET systems.[7] Such results bring out three key features that determine ET rates in DBA systems: the bridge chemical structure, the DBA energy gap, and the bridge length or the donor−acceptor distance. In particular, it is often assumed that the dependence of the ET rate (k_{ET}) on the donor−acceptor distance (R_{DA}) is of the form

$$k_{ET} = A(T) \exp(-\beta R_{DA}) \tag{1}$$

where $A(T)$ is a temperature-dependent prefactor and β is a constant characterizing the bridge and DA pair. It is currently accepted that the value of β is mostly sensitive to the structure of the bridging media,[8] with highly conjugated organic bridges having the smallest β values ($0.2-0.6$ Å^{-1})[7,9−18] and with free space being characterized by a β value of ~ 2.0 A^{-1}.[3] Lying between these two regimes are many motifs, both synthetic and natural, including cytochromes and docked proteins,[19−24] DNA,[25−32] and saturated organic molecules.[33−37] Each displays its own characteristic range of β values and, hence, its own time scales and distance dependencies of ET.

The exponential dependence, eq 1, of the ET rate on R_{DA} has been derived using many different methodologies,[38−41] the earliest of which dates back to McConnell's use of perturbation theory to describe electron exchange rates in organic complexes.[42] This regime of ET is known as superexchange,[43−46] and it is characterized by the absence of any population physically residing on the bridge during the ET process. In terms of the simple dynamical scheme for bridged charge separation reactions, DBA → D^+B^-A → D^+BA^-, the intermediate state D^+B^-A is a virtual state that is not physically populated. In the opposite regime, the electron actually occupies the bridge,

† Part of the special issue "Harvey Scher Festschrift".
‡ Northwestern University.
§ Argonne National Laboratory.

10.1021/jp993260f CCC: $19.00
Published on Web 03/24/2000

that is, the state D^+B^-A is physically occupied, and diffusion or sequential hopping of the electron between bridge sites may become rate-limiting. In this limit, the distance dependence of the electron-transfer process is characterized by Ohm's law, specifically

$$k_{ET} \propto \frac{1}{N} \tag{2}$$

where N is the number of bridge sites between the donor and the acceptor. We have recently pointed out[47] that, in the intermediate regime between the behaviors described by eqs 1 and 2, the rate may appear to be independent of N in some range. Plausible, but inconclusive, experimental evidence for the existence of this regime has recently been obtained for a series of molecules based on organic donors and acceptors bridged by short chain oligomers of the conducting polymer poly(*p*-phenylenevinylene).[48]

It is important to realize that, because the dynamics described by eq 2 correspond to the electron physically residing on the bridge, the corresponding rate should be thermally activated, that is, $k_{ET} \sim N^{-1} \exp[-(k_B T)^{-1}\Delta E]$, where ΔE is the (positive) D−B energy gap. In the opposite case when $\Delta E \leq 0$, that is, when the donor level is higher in energy than the lowest bridge level, the bridge can become populated without thermal activation. Phase loss leading to sequential migration may take place in this case because of the irregular character of the coupling between different vibronic levels in the D, B, and A entities.[49]

The transition between the superexchange (tunneling) and the sequential hopping regimes has attracted some attention recently.[50,51] In particular, Felts, Pollard, and Friesner[52] have investigated this issue in the framework of the Redfield density matrix theory,[53] and Mukamel and collaborators have advanced a more elaborate density matrix formalism using higher-order correlation functions for the system−thermal bath coupling.[54] Other potentially useful formulations of reduced equations of motion for a quantum system in a thermal environment have been developed recently,[55−58] although they have not been applied to problems of the type considered here. These investigations focus on the time-dependent process represented as an initial value problem: The electron is on the donor at $t = 0$, and the subsequent time evolution is followed. We have recently presented a simpler phenomenological analysis of the steady-state problem.[47] Our approach also starts from the Liouville equation for the reduced density matrix of the DBA system, but it focuses on the steady-state flux as the principal observable. Physically, this situation corresponds to molecular junctions between two metal contacts, where the steady-state current is monitored as a function of applied voltage. Other approaches to dephasing effects on electron transmission have been used in the nano-junction physics literature.[59,60]

The purpose of the present paper is to extend the steady-state density matrix approach to the DBA ET problem in several directions. First, we replace the phenomenological density matrix equations of ref 47, where the thermal relaxation rates were introduced as phenomenological constants, by a form in which the thermal rates are given by microscopic expressions involving Fourier transforms of bath correlation functions. This modification makes it possible to account correctly for the order of magnitude of these rates and their dependence on the energy gap and the temperature. Second, we take into account the possibility of thermal relaxation on the bridge by assigning more than one level to each bridge site. The resulting model for the steady-state theory described here becomes equivalent to that used in the time-dependent theories of refs 52 and 54, although we use a simpler, two-level rather than harmonic-oscillator model for the relaxation within the bridge sites. We then use this model to investigate the effect of thermal relaxation on the nature of the ET process. In addition, we address several other issues: First, we investigate the correspondence between steady-state and transient phenomena, in particular the relation between the steady-state rate and the rate obtained from transient measurements. Second, we study the transition from coherent tunneling via the superexchange mechanism to incoherent hopping for increasing thermal relaxation and increasing bridge length. The nature of the intermediate regime in which the computed flux appears to be bridge-length-independent is elucidated, and the possible consequences of the existence of such a regime are discussed. The steady-state formulation of the ET problem is directly applicable to steady-state experiments, such as current vs voltage (i.e. conductance) measurements. We have recently shown[61] that the Landauer formula[62] that connects the conductance of a junction to its transmission properties can be generalized to situations involving thermal relaxation in the barrier. We use this generalization to estimate the relationship between the electron-transfer rate associated with a given bridge and its conductance. Finally, we discuss possible experimental methods for determining the route (thermal or nonthermal) by which the process of electron transmission takes place.

In the next section, we describe the model used in the present discussion of bridge-mediated electron transfer with thermal relaxation. Following this, in section 3, we derive approximate equations of motion for the reduced density matrix of the molecular system and formally solve them for the steady-state rate. The procedure used and the resulting equations are similar to the Redfield theory; however, we repeat the derivation in order to emphasize some subtle issues associated with the application of this type of theory to steady-state nonresonant processes. Section 4 discusses the relationship between the steady-state rate and its counterpart obtained from the transient process following a pulse preparation of the donor level. Numerical results for some model systems and a discussion of the dependence of the computed rate on our model parameters are provided in section 5. Section 6 discusses the implication of these results for the conductance of a junction constructed with a given molecular bridge between two metal contacts. In section 7, we discuss possible ways of distinguishing experimentally between the thermal and the tunneling routes in bridge-mediated ET processes. Some concluding remarks are made in section 8.

2. The Molecular Model

In the present discussion, we limit ourselves to a minimal model that can describe the physical process under discussion, specifically, bridge-mediated electron transfer between given donor and acceptor levels and the factors that affect it: electronic coupling; thermal interactions that lead to dephasing within the bridge and between bridge and the donor/acceptor levels; thermal relaxation between occupied bridge levels; possible losses to competing channels; and, when relevant, initial and final electron reservoirs that correspond to metal contacts. We bear in mind that the donor and acceptor "levels" are, in reality, manifolds of vibronic levels associated with donor and acceptor electronic states and that, similarly, each bridge site corresponds to an intermediate electronic state with its own vibronic manifolds. This important aspect of the problem is simplified in our model (Figure 1). Panel a depicts the simplest superexchange model that consists of a single donor level, a single

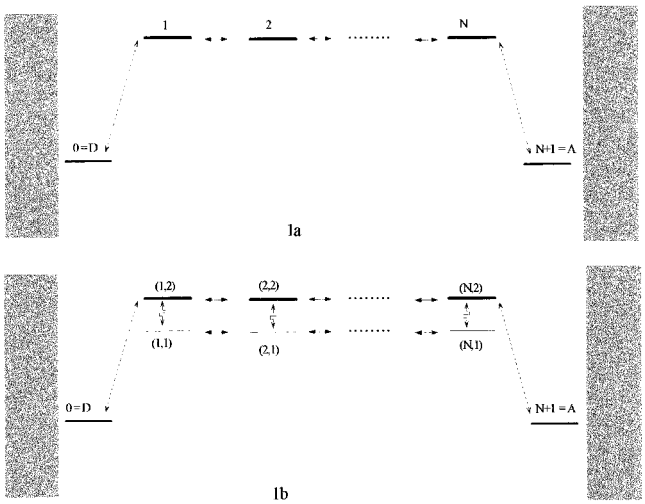

Figure 1. Schematic representation of the models A (upper panel) and B (lower panel) that are discussed in the text. D and A represent donor and acceptor levels (also marked 0 and $N + 1$). The other levels correspond to the bridge. Double arrows represent electronic coupling (the wavy double arrows in model B represent thermal relaxation). The continua on the left and right correspond to the source that maintains the population in the donor and the sink that removes population from the acceptor. In a metal−molecular layer−metal junction, these continua are quasi-free electron states in the metal. In this case, D and A may denote the positions of the corresponding Fermi energies.

acceptor level, and a single intermediate level for each bridge site; it will be referred to as model A. The continuous manifolds on the two sides of this figure correspond to electronic states of metal contacts if the model is to describe a metal−molecule−metal junction. In ref 47, we analyzed the effect of additional dephasing interactions on the charge-transfer dynamics associated with this model. We, as well as others,[52,54] have found that, in this case, a thermal channel for electron transport may open, in which the electron physically occupies the bridge. When this mechanism is important, we must account for thermal transitions between bridge levels, as well as for thermal dephasing on the bridge. In most cases, the strongest electronic coupling between donor (acceptor) and bridge levels, as well as electronic coupling between bridge levels, involves higher vibrational levels of these sites. When the bridge is physically occupied, thermal relaxation between these levels may affect the electron transport processes. To account for this effect, we consider the model of Figure 1b with two levels per bridge site, which we will call model B. The levels marked by bold horizontal lines are those that appear in Figure 1a. The levels marked by thin horizontal lines are lower vibrational levels of the bridge that are assumed to couple relatively weakly to the donor/acceptor levels and also among themselves. Note that models used by other workers[52,54] also consider higher vibrational levels both in the donor−acceptor sites and in the bridge sites. Our minimal model is sufficient for a qualitative discussion of the effect of thermal relaxation on bridge-mediated electron transfer, and its simplicity makes it possible to elucidate the nature of the effects observed. At the same time, the formulation given below may be generalized to more sophisticated models if desired.

In the discussion that follows, we use Latin indices to denote donor, acceptor, and bridge sites and Greek indices to denote vibrational levels within each site. The donor level is denoted by D or $n = 0$, the acceptor level is denoted by A or $n = N + 1$, and the bridge sites are denoted $n = 1, 2, ..., N$. The Hamiltonian for the overall system is

$$H = H_M + H_B + F \tag{3}$$

where H_B is the Hamiltonian of the free thermal environment (or bath). H_M is the molecular Hamiltonian, which is further separated according to

$$H_M = H_0 + V \tag{4}$$

where H_0 contains the local Hamiltonian for the donor, acceptor, and bridge molecular units

$$H_0 = E_D|D\rangle\langle D| + E_A|A\rangle\langle A| + \sum_{n=1}^{N}\sum_{\alpha=1}^{2} E_{n\alpha}|n\alpha\rangle\langle n\alpha| \tag{5}$$

and where V is the molecular coupling responsible for the ET process in the isolated system. For this interaction, we assume the usual nearest-neighbors coupling form

$$V = \sum_{\alpha=1}^{2}[V_{0,1\alpha}|0\rangle\langle 1\alpha| + V_{1\alpha,0}|1\alpha\rangle\langle 0| + V_{N\alpha,N+1}|N\alpha\rangle\langle N + 1| + V_{N+1,N\alpha}|N+1\rangle\langle N\alpha|] + \sum_{n=1}^{N-1}\sum_{\alpha=1}^{2}\sum_{\alpha'=1}^{2}[V_{n\alpha',(n+1)\alpha'}|n\alpha\rangle\langle(n+1)\alpha'| + V_{(n+1)\alpha',n\alpha}|(n+1)\alpha'\rangle\langle n\alpha|] \tag{6}$$

Finally, the molecule−bath coupling H_{MB} takes the form

$$F = \sum_{n=1}^{N}\sum_{\alpha=1}^{2}\sum_{\alpha'=1}^{2}(F)_{n\alpha,n\alpha'}|n\alpha\rangle\langle n\alpha'| \tag{7}$$

where the molecular matrix elements of F are operators in the bath coordinates.

The model just described, model B, has already been simplified by taking a tight-binding form for the interaction and by limiting the number of bridge levels to two per site. We have also disregarded the vibronic structure of the donor (D) and acceptor (A) electronic states. In realistic applications, the result should be averaged over a distribution of donor states. On the opposite side of the system, we will ensure irreversibility by assigning a width Γ_A to the acceptor level. Γ_A signifies that $|A\rangle$ actually represents a continuum of states: either the vibrational quasi-continuum of the acceptor and the solvent in a regular ET process or a continuum of quasi-free electron states in case of a metal contact. Finally, the form of eq 7 implies that the thermal bath does not couple different electronic states and that it induces relaxation and dephasing only within the local site. Given this assumption, we may exclude, without further loss of generality, the donor and acceptor levels from the sum in eq 7, as was done above.

Given the Hamiltonian in eqs 3−7, we will consider the time evolution of the reduced density operator of the molecular system, $\sigma(t) = \mathrm{Tr}_B\rho(t)$, where $\rho(t)$ is the density operator of the overall molecule−bath system and where Tr_B is a trace over all bath states.

Assuming that

$$\langle F\rangle_B = \mathrm{Tr}(\rho_B F) = 0 \tag{8}$$

where $\rho_B = (\mathrm{Tr}_B e^{-H_B/k_BT})^{-1}e^{-H_B/k_BT}$ is the density operator of the thermal environment, standard theory (see section 3) leads to equations of motion for the matrix elements of σ with thermal relaxation coefficients expressed as Fourier−Laplace transforms of bath correlation functions. The latter are of the form

$$C_{n\alpha_1,n\alpha_2,n'\alpha_3,n'\alpha_4}(t) = \langle(\tilde{F}(t))_{n\alpha_1,n\alpha_2}(\tilde{F}(0))_{n'\alpha_3,n'\alpha_4}\rangle_B \quad (9)$$

where $\tilde{F}(t) = e^{iH_B t}Fe^{-iH_B t}$. We will make the additional assumption that no correlations exist between system−bath interactions associated with different sites, that is, only terms with $n = n'$ contribute in eq 9. The rationale for this model assumption lies in the local nature of the states n. We essentially assume that the perturbations induced in the bath when the electron resides in sites n and n' ($n \neq n'$) are associated with different, uncorrelated, bath degrees of freedom.

Next we derive approximate equations of motion for the reduced density matrix of the molecular system and show how the steady-state rate can be computed from these equations.

3. Reduced Equations of Motion

Starting with the Liouville equation for the density operator ρ of the overall molecule−bath system (working with units for which $\hbar = 1$)

$$\dot{\rho} = -i[H,\rho] \quad (10)$$

with H given by eqs 3−7, we proceed as usual to derive the corresponding equation of motion for the reduced molecular density operator $\sigma = \mathrm{Tr}_B\rho$. Standard approximations, which rely on the assumptions that V and F are small relative to the characteristic energy spacing of the molecular system and that ρ is approximated well by the product $\rho_B\sigma(t)$, lead[63] to the Redfield-type equation

$$\begin{aligned}\dot{\sigma}_{jk} = &-i\omega_{jk}\sigma_{jk} - i[V,\sigma]_{jk} - \\ &\int_0^t dt' \sum_{lm}\{\langle\tilde{F}_{jl}(t-t')\tilde{F}_{lm}(0)\rangle e^{-i\omega_{lk}(t-t')}\sigma_{mk}(t') - \\ &\langle\tilde{F}_{mk}(0)\tilde{F}_{jl}(t-t')\rangle e^{-i\omega_{lk}(t-t')}\sigma_{lm}(t') - \\ &\langle\tilde{F}_{mk}(t-t')\tilde{F}_{jl}(0)\rangle e^{-i\omega_{jm}(t-t')}\sigma_{lm}(t') + \\ &\langle\tilde{F}_{ml}(0)\tilde{F}_{lk}(t-t')\rangle e^{-i\omega_{jl}(t-t')}\sigma_{jm}(t')\} \quad (11)\end{aligned}$$

where

$$\tilde{F}(t) = e^{iH_B t}Fe^{-iH_B t} \quad (12)$$

and where $\langle\ \rangle$ denotes an average over a thermal distribution of the bath. We will later supplement this equation with phenomenological damping terms that are associated with the decay of the acceptor level, as discussed above. Equation 11 is further simplified if the bath correlation functions are assumed to decay quickly, so that t' is close to t. The standard Redfield equations[64] are obtained by substituting

$$\sigma_{jk}(t') = \sigma_{jk}(t)e^{i\omega_{jk}(t-t')} \quad (13)$$

in all terms in the integral of eq 11 and then setting the upper integration limit to infinity. This substitution leads to

$$\begin{aligned}\dot{\sigma}_{jk} = &-i\omega_{jk}\sigma_{jk} - i[V,\sigma]_{jk} + \\ &\sum_{lm}\{\sigma_{lm}(t)\int_0^\infty d\tau[\langle\tilde{F}_{mk}(0)\tilde{F}_{jl}(\tau)\rangle e^{-i\omega_{mk}\tau} + \\ &\langle\tilde{F}_{mk}(\tau)\tilde{F}_{jl}(0)\rangle e^{-i\omega_{jl}\tau}] - \sigma_{mk}(t)\int_0^\infty d\tau\langle\tilde{F}_{jl}(\tau)\tilde{F}_{lm}(0)\rangle e^{-i\omega_{lm}\tau} - \\ &\sigma_{jm}(t)\int_0^\infty d\tau\langle\tilde{F}_{ml}(0)\tilde{F}_{lk}(\tau)\rangle e^{-i\omega_{ml}\tau}\} \quad (14)\end{aligned}$$

Alternatively, *at steady state*, σ is time independent. Equation 11 then becomes

$$\begin{aligned}0 = -i\omega_{jk}\sigma_{jk} - i[V,\sigma]_{jk} = \\ \sum_{lm}\{\sigma_{lm}\int_0^\infty d\tau[\langle\tilde{F}_{mk}(0)\tilde{F}_{jl}(\tau)\rangle e^{-i\omega_{lk}\tau} + \langle\tilde{F}_{mk}(\tau)\tilde{F}_{jl}(0)\rangle e^{-i\omega_{jm}\tau}] - \\ \sigma_{mk}\int_0^\infty d\tau\langle\tilde{F}_{jl}(\tau)\tilde{F}_{lm}(0)\rangle e^{-i\omega_{lk}\tau} - \\ \sigma_{jm}\int_0^\infty d\tau\langle\tilde{F}_{ml}(0)\tilde{F}_{lk}(\tau)\rangle e^{-i\omega_{jl}\tau}\} \quad (15)\end{aligned}$$

Equation 15 is obviously different from the steady-state limit of eq 14; however, eq 14 will yield the correct steady-state solution in the common case where this steady state is characterized by zero nondiagonal elements of σ. In the examples discussed in section 5 below, we typically find that, at steady state, $\sum_{i\neq j}|\sigma_{ij}|^2/\sum_i\sigma_{ii}^2 \leq 10^{-2}$, implying that results based on eqs 14 and 15 are practically identical.

It has been noticed,[65] but not widely recognized, that eq 14 (and eq 15) does not yield the correct long-time limit, that is, a Boltzmann population distribution, in a model of a closed system (no damping terms added to eqs 11, 14, and 15) that is characterized by diagonal coupling to the thermal environment ($F_{jk} = F_{jj}\delta_{jk}$) if the molecular coupling V is non-zero.[73]

This result is an artifact of the low-order approximation used in Redfield-type theories and can be avoided if we stick to the representation that diagonalizes H_M in eq 4, that is, if we use eq 14 or 15 for the case $V = 0$.[64] For this reason, we will also use the molecular basis with eqs 14 and 15, that is, we will use these equations with $V = 0$ and with ω_{ij} defined as the difference between eigenvalues of H_M. However, because our boundary conditions and assumptions about the correlation properties of F_{ij} are given in the local basis (eigenfunctions of H_0), we must transform back and forth between these representations. In this process, we use the transformation equations summarized in Appendix A. Our procedure, therefore, proceeds along the following steps:

(1) The model is defined in terms of the local basis, as presented in section 2.

(2) The Hamiltonian is rewritten in the molecular basis representation (see Appendix A), that is, we replace the representation in eq A1 by the form in eq A2 using eqs A5 and A7. All thermal operators $\bar{F}_{vv'}$ in this representation (see Appendix A) will now be non-zero and mutually correlated.

(3) The reduced equations of motion are derived in this molecular basis representation, leading to equations of the forms in eqs 14 and (for steady state) 15 with $V = 0$. These equations are of the general form of eq A4 (with $\dot{\sigma} = 0$ in the steady-state case).

(4) The resulting equations of motion for the molecular density matrix in the molecular basis representation are transformed back to the local basis representation using eqs A5, A6, and A8, leading to equations of the form of eq A3 (with $\dot{\sigma} = 0$ in steady state). It is important to note that the resulting equations are different from those that would be obtained by applying the Redfield procedure to the original Hamiltonian (eq A1), because the procedures for transforming between the molecular and local bases and for reducing the density matrix equations of motion do not commute with each other.

(5) After step 4 has been executed, we obtain the equations of motion for the molecular density matrix in the local representation in the form (using the notation of Appendix A)

$$\frac{d\sigma_{nn'}}{dt} = -i\omega_{nn'}\sigma_{nn'} - i[V,\sigma]_{nn'} + \sum_{n_1}\sum_{n_2}\tilde{R}_{nn'n_1n_2}\sigma_{n_1n_2} \quad (16)$$

where the elements of $\tilde{R}$ are linear combinations of the integrals

appearing in eq 14, and the corresponding steady-state equations

$$-\mathrm{i}\omega_{nn'}\sigma_{nn'} - \mathrm{i}[V,\sigma]_{nn'} + \sum_{n_1}\sum_{n_2}\tilde{R}_{nn'n_1n_2}\sigma_{n_1n_2} = J_{nn'} \quad (17)$$

where the elements of $\tilde{R}$ are the same linear combinations, but of the corresponding integrals appearing in eq 15, and where the terms $J_{nn'}$ define our boundary conditions. Note that the indices n in eq 17 stand for the combination $(n\alpha)$ that defines the vibronic states in the model described in section 2. In the present work, we study the steady state associated with the following boundary conditions:

$$J_{\mathrm{DD}} = -J$$
$$J_{\mathrm{AA}} = \Gamma_{\mathrm{A}}\sigma_{\mathrm{AA}}$$
$$J_{\mathrm{A}n} = \frac{1}{2}\Gamma_{\mathrm{A}}\sigma_{\mathrm{A}n};\ J_{n\mathrm{A}} = \frac{1}{2}\Gamma_{\mathrm{A}}\sigma_{n\mathrm{A}} \quad (18)$$
$$J_{nn'} = 0 \text{ for } n, n' \neq \mathrm{A}$$

where J is the steady-state flux, and where we assume that the population in the acceptor state A decays with a given rate Γ_{A}.[74] With this **J**, eq 17 constitutes a set of $(N+2)\times(N+2)$ (for model A) or $(2N+2)\times(2N+2)$ (for model B) linear algebraic equation that yield all $\sigma_{nn'}$ in terms of J and the molecular and thermal parameters. In particular, the σ_{AA} at steady state is J/Γ_{A}, and the σ_{DD} resulting from this calculation is used to calculate the steady-state rate according to

$$k_{\mathrm{ss}} = J/\sigma_{\mathrm{DD}} \quad (19)$$

An alternative procedure that yields the same result is to disregard the equation associated with $\dot{\sigma}_{\mathrm{DD}}$, impose a constant σ_{DD} and the damping terms associated with Γ_{A} on the other equations, and solve the resulting set of equations for $\sigma_{nn'}$ in terms of the given σ_{DD}. In particular, we find the steady-state value of σ_{AA}. The steady-state rate is then

$$k_{\mathrm{ss}} = \frac{\Gamma_{\mathrm{A}}\sigma_{\mathrm{AA}}}{\sigma_{\mathrm{DD}}} \quad (20)$$

4. Steady-State vs Transient Dynamics

The steady-state rate k_{ss} defined by eq 20 corresponds to a measurement of the current in the molecular junction where the donor−bridge−acceptor model defined in section 2 connects two electron reservoirs, that is, metal contacts. The reservoir associated with the "donor" keeps the population σ_{DD} of the latter constant, while the reservoir associated with the acceptor provides the damping mechanism represented by the rate Γ_{A}. A different, common experimental situation corresponds to the initial value problem in which the donor state is prepared at $t = 0$ (usually by an optical excitation). In this transient mode, the long-time evolution of the signal (for example, donor fluorescence) is fitted to an exponential $\exp(-k_{\mathrm{LT}}t)$ to yield the rate k_{LT}. Theoretically, this rate is assigned to the lowest eigenvalue of the tetradic matrix that describes the time evolution, including relaxation, of the reduced density matrix of the system. It is interesting to compare the rates computed in these different ways and, in particular, to ask if and under what conditions they can be equal to each other.

It is important to realize that a given dynamic model, such as a set of coupled molecular levels subject to thermal relaxation and dephasing interactions, can describe different steady-state processes depending on the boundary conditions, that is, depending on the details of the source and sink processes. Similarly, the "long-time rate" associated with a transient experiment described by the same model depends on the details of the initially prepared state and of the monitored signal. For definiteness, we will focus on the model of Figure 1a and will consider the steady-state rate given by eq 19 or 20, which is associated with a given population in the donor state and a given decay rate of the acceptor state. The corresponding transient experiment is associated with the initial condition $\sigma_{\mathrm{DD}}(t=0) = 1$, $\sigma_{ij}(t=0) = 0$ (i and/or $j \neq$ D). We use a vector−matrix notation for the rate equations

$$\frac{\mathrm{d}\mathbf{C}}{\mathrm{d}t} = \mathbf{A}\mathbf{C} \quad (21)$$

where the elements C_k $[k = 0, ..., (N+1)^2]$ correspond to elements σ_{ij} of the molecular density matrix, and the elements of **A** are the corresponding energy differences and relaxation/dephasing rates. In particular, we take $C_0 = \sigma_{\mathrm{DD}}$ and $C_{(N+1)^2} = \sigma_{\mathrm{AA}}$. Let the set of right and left eigenvectors of **A** be $|\mathbf{v}_k\rangle$ and $\langle\mathbf{v}_k|$ with the corresponding eigenvalues γ_k, all with negative real parts, and let $|\mathbf{v}_{\mathrm{s}}\rangle$ be the eigenvector corresponding to the eigenvalue γ_{s} with the smallest absolute real part. In the discussion that follows, we assume that this eigenvalue is real. Therefore,

$$k_{\mathrm{LT}} = -\gamma_{\mathrm{s}} \quad (22)$$

Consider now the steady-state rate associated with the boundary conditions defined above and given explicitly in eq 18. The corresponding elements of $\mathbf{C}_{\mathrm{ss}}$ can be obtained from

$$\mathbf{A}\mathbf{C}_{\mathrm{ss}} + \mathbf{J} = 0 \quad (23)$$

where the vector **J** is given by

$$J_k = J\delta_{k0} \quad (24)$$

J is the steady-state flux through the system. We obtain

$$\mathbf{C}_{\mathrm{ss}} = -\sum_j \frac{1}{\gamma_j}|\mathbf{v}_j\rangle\langle\mathbf{v}_j|\mathbf{J}\rangle \cong -\frac{1}{\gamma_{\mathrm{s}}}|\mathbf{v}_{\mathrm{s}}\rangle\langle\mathbf{v}_{\mathrm{s}}|\mathbf{J}\rangle \quad (25)$$

The last approximation is valid if γ_{s} is considerably smaller than all other eigenvalues of **A**. The steady-state rate is

$$k_{\mathrm{ss}} = \frac{J}{C_0^{\mathrm{ss}}} = -\gamma_{\mathrm{s}}\langle\mathbf{I}|\mathbf{v}_{\mathrm{s}}\rangle\langle\mathbf{v}_{\mathrm{s}}|\mathbf{I}\rangle \quad (26)$$

where $|\mathbf{I}\rangle$ is the transpose of (1, 0, ..., 0), that is, the vector $\mathbf{C}(t=0)$. Equations 22 and 26 imply that $k_{\mathrm{ss}} = k_{\mathrm{LT}}$ provided that

$$\mathbf{C}_{\mathrm{ss}} \approx |\mathbf{v}_{\mathrm{s}}\rangle \approx \begin{pmatrix} 1 \\ 0 \\ \vdots \\ 0 \end{pmatrix} \quad (27)$$

namely, provided that at steady state $\sigma_{\mathrm{DD}} \cong 1$ and $\sigma_{ij} \ll 1$ for $(ij) \neq$ (DD). Note that, in the transient experiment, this is also the condition that k_{LT} is a meaningful rate of the process. For this to be true, a quasi-steady state must be reached while most of the population is still in the donor state. This condition is often satisfied in a donor−bridge−acceptor system provided

that the energy separation between the donor and bridge is not too small. Some examples are shown in the next section.

5. Numerical Results and Discussion

The numerical results presented below are intended to illustrate the general phenomenology associated with the competition between the coherent tunneling and the incoherent hopping mechanisms that, in principle, coexist in bridge-mediated electron transfer in condensed environments. We focus on the dependencies on the energy gap, the bridge length, the temperature, and the strength of the thermal interaction. In addition, we study some theoretical issues, including the effect of the finite bath correlation time and the similarity between the rates k_{LT} and k_{ss}, as defined in section 4.

In the discussion that follows, all non-zero bath correlation functions that appear in eqs 14 and 15 are assigned the Gaussian form $(\tau_c\sqrt{\pi})^{-1}\kappa e^{-(t/\tau_c)^2}$, where $\tau_c \equiv \gamma_c^{-1}$ is the bath correlation time and κ measures the associated relaxation or dephasing rate. The detailed-balance property of the quantum correlation functions is incorporated, so that

$$\int_{-\infty}^{\infty} dt e^{i\omega t}\langle F(0)F(t)\rangle = \begin{cases} \kappa e^{-(1/2\tau_c\omega)^2}; & \omega \geq 0 \\ e^{-|\omega|/k_B T}\kappa e^{-(1/2\tau_c\omega)^2}; & \omega < 0 \end{cases} \quad (28)$$

In reality, the parameter κ may have different magnitudes for different correlation functions, and the ω dependence in eq 28 can be better represented by a function other than a Gaussian.[75] However, the present model contains the basic features affecting the process, the magnitude and the spectrum of the relevant correlation functions.

In the following presentation, we use two molecular models. The familiar model consisting of one level per bridge site (Figure 1a), referred to as model A, is used because of the prominent role it has played in describing bridge-assisted electron transfer. Thermal relaxation effects appear in this model as dephasing of the bridge levels. When the system is close to resonance, and/or when the bridge may be thermally populated, the vibronic level structure of the donor, acceptor, and bridge sites may have an essential effect on the dynamics. As described in section 2, we represent this situation (model B, Figure 1b) by two vibronic levels per bridge site. Here, thermal relaxation in the bridge can cause both dephasing and population relaxation, but in the results shown below, only population relaxation between bridge levels (on the same site) was taken, using the same parameters κ and τ_c as in the dephasing interactions in model A. Note that, as already emphasized in section 3, the assignment of thermal interaction terms as corresponding to dephasing or population relaxation depends on the representation used, and the above statements refer to the local representation. We also emphasize that none of the qualitative aspects of the observations described below depend on these particular details of the model.

Unless otherwise stated, the following set of parameters is used for model A: E_0 ($\equiv E_D$) $= E_{N+1}$ ($= E_A$), $\Delta E \equiv E_n - E_0 = 3000$ cm^{-1} ($n = 1, 2, ..., N$), $V_{n,n\pm1} = 300$ cm^{-1}, $\Gamma_A = 400$ cm^{-1}, $\tau_c^{-1} = 600$ cm^{-1}, $\kappa = 100$ cm^{-1}, and $T = 300$ K. For model B, each bridge level n is replaced by two levels ($n\alpha$), $n = 1, 2, ..., N$; $\alpha = 1, 2$. The same parameters as in model A are used for the donor, the acceptor, and the *upper* bridge levels, while each lower bridge level ($n1$) is placed 500 cm^{-1} below the corresponding higher level ($n2$), that is, 2500 cm^{-1} above the donor and acceptor levels. In addition, each lower bridge level is coupled thermally to the level above it via the term $F_{n1,n2}|n1\rangle\langle n2| + h.c.$ in the Hamiltonian. The molecular coupling involving these lower levels is assumed to vanish (that is, $V_{0,11} = V_{n1,n'\alpha'} = V_{n\alpha,n'1} = V_{N1,N+1} = 0$ for all $n, n' = 1, 2, ..., N$ and $\alpha, \alpha' = 1, 2$). This choice of coupling implies that the electron can be transferred only along the upper bridge levels. It is an enhancement of the common situation, where vibronic coupling between different sites is maximized at some excess vibrational energy (for which the corresponding electronic potential surfaces cross). Again, none of the qualitative conclusions reached below depends on these details.

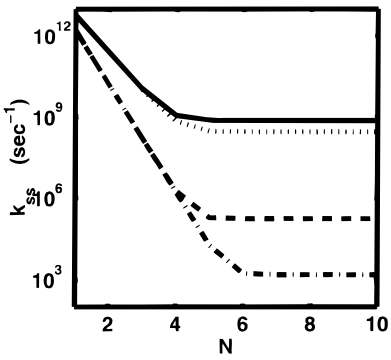

Figure 2. Steady-state rate, k_{ss}, as a function of the bridge length N for model A (see text). Solid line: $\Delta E = 1500$ cm^{-1} and $\tau_c = 0$. Dotted line: $\Delta E = 1500$ cm^{-1} and $\tau_c^{-1} = 600$ cm^{-1}. Dashed line: $\Delta E = 3000$ cm^{-1} and $\tau_c = 0$. Dashed-dotted line: $\Delta E = 3000$ cm^{-1} and $\tau_c^{-1} = 600$ cm^{-1}. The temperature is 300 K in all cases.

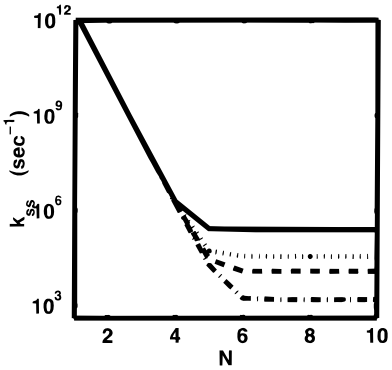

Figure 3. Same as Figure 2, now comparing results for models A and B for the case $\tau_c^{-1} = 600$ cm^{-1}. Solid line: model B, $T = 400$ K. Dotted line: model A, $T = 400$ K. Dashed line: model B, $T = 300$ K. Dashed-dotted line (identical to same line in Figure 2): model A, $T = 300$ K.

Figure 2 shows the steady-state rate, k_{ss}, as a function of the bridge length N for model A. Shown are results for $\Delta E = 3000$ and 1500 cm^{-1} for the fast thermal bath limit ($\tau_c = 0$) and for a finite bath response time, $\tau_c^{-1} = 600$ cm^{-1}. All results are characterized by the same qualitative behavior, showing a transition from exponential dependence on the bridge length [$k_{ss} \sim (V/\Delta E)^{2N}$], which characterizes the tunneling mechanism, to almost no dependence on this length at some crossover value of N (see discussion below). In addition, taking into account the finite time of the bath response strongly reduces the effect of thermal relaxation, inhibits the onset of the incoherent hopping mechanism, and reduces the rate for large N, as could be anticipated from eq 28.

Figure 3 compares results of similar calculations done with models A and B. Here, results are shown for $\Delta E = 3000$ cm^{-1} for two temperatures, $T = 300$ and 400 K. Note that the dependence of the parameters κ and τ_c^{-1} on temperature is disregarded in making this comparison, although, in reality, both are expected to increase with T in this range. We see that, at the same temperature, the rate associated with model B is about an order of magnitude larger than the corresponding rate of

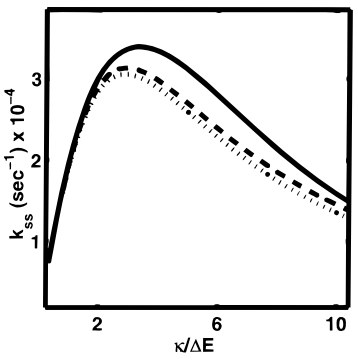

Figure 4. Steady-state rate, k_{ss}, as a function of the dephasing rate κ for model A, for bridge lengths $N = 6$ (solid line), $N = 7$ (dashed line), and $N = 8$ (dotted line). k_{ss} is plotted against the ratio between the dephasing rate κ and the energy gap ΔE for $\Delta E = 3000$ cm^{-1} and $\tau_c^{-1} = 600$ cm^{-1}.

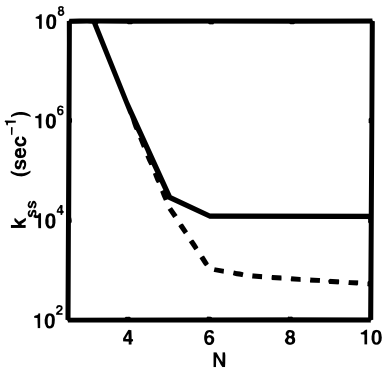

Figure 5. Steady-state rate, k_{ss}, as a function of bridge length N for model B (solid line) and for the same model modified by adding a damping term $\Gamma_B = 2$ cm^{-1} to the dynamics of the lower bridge level (dashed line). See text for details.

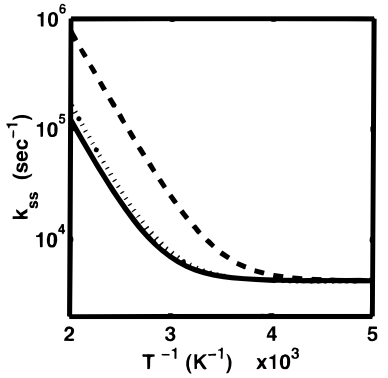

Figure 6. Steady-state rate, k_{ss}, plotted against T^{-1} for a bridge of length $N = 5$. Solid line: model A. Dashed line: model B. Dotted line: model B modified by assigning damping terms $\Gamma_B = 2$ cm^{-1} to the lower bridge levels.

model A, even though, with our choice of coupling in the local representation, the lower bridge levels in model B should not carry flux. This finding may seem odd at first, as one might have expected that, because electron transition via the lower bridge levels is blocked by our choice of coupling scheme, these levels could function as traps that slow the transfer rate. However, such trapping does not occur at steady state because, by definition, the rates for population and depopulation of these levels are equal in this situation. The strength of the system−environment coupling (expressed by the parameter κ, eq 28) is not an easily controlled parameter;[76] however, it has played an important role in other contexts, such as discussions of barrier crossing rates as functions of solvent viscosity.[66] Figure 4 shows, for model A, the dependence of k_{ss} on κ for several chain lengths N above the crossover to hopping. In this regime of N, a familiar dependence is observed: k_{ss} increases with κ for small κ and decreases with κ in the "overdamped", large κ limit.†[77] Note that, in the "underdamped limit", $\kappa \ll \Delta E$, the rate is almost independent of N. We return to this observation later.

One could infer from the results shown above that thermal population of the bridge is always advantageous in promoting long-range energy transfer. As a word of caution, we note that, although tunneling is associated with very short bridge traversal times (and consequently, with low relative yields of competitive processes), physical occupation of the bridge by the transmitting electron can increase competition from other channels that might reduce the yield of electron transmission. The most important effect may be a deflection of an incoming electron from the bridge region by the repulsive interaction with another electron that already occupies the bridge. The present one-electron model cannot describe this Coulomb blockade effect. Instead, we consider in Figure 5 the effect of associating, in model B, a small loss term with the time evolution of the lower bridge levels [specifically, we add $-\Gamma_B\sigma_{n1,n1}$, $-^1/_2\Gamma_B\sigma_{j,n1}$, and $-^1/_2\Gamma_B\sigma_{n1,j}$ ($j \neq n1$) to the equations of motion for $\dot{\sigma}_{n1,n1}$, $\dot{\sigma}_{j,n1}$, and $\dot{\sigma}_{n1,j}$, respectively]. Such a loss term may result, for example, from the presence of other carrier acceptors in the system.[67] Figure 5 shows the resulting plot of k_{ss} vs N for model B, comparing the cases $\Gamma_B = 0$ to $\Gamma_B = 2$ cm^{-1}. Obviously, the effect of adding this damping channel is to reduce the rate associated with the hopping regime, and this reduction becomes more pronounced for longer chains. In fact, if such a constant loss term is associated with each bridge site, we expect an exponential falloff of the transmission rate with chain length (see Appendix B), as indeed seen in Figure 5 (dashed line). This loss is usually expected to be small, so the associated exponential decay with chain length is expected to be much weaker than that found in the coherent tunneling (superexchange) regime of eq 1. It has apparently been seen experimentally in hole-transfer processes in DNA.[67]

The temperature dependence of the steady-state rate is depicted in Figure 6. Shown are Arrhenius plots, k_{ss} vs T^{-1}, for model A, model B, and model B modified by adding the loss term $\Gamma_B = 2$ cm^{-1} to the dynamics of the lower bridge levels, as described above. We see the characteristic transition from temperature-independent behavior at low T, where the process is dominated by tunneling, to Arrhenius behavior at high T. The activation energies characterizing the Arrhenius behavior are found to be approximately 2600 cm^{-1} for model A and 2500 cm^{-1} for model B. The lowering of the activation energy relative to the zero order gap, ΔE, is associated with the presence of the electronic coupling V, which will make the actual gap smaller for some of the states that diagonalize H_M (eq 4).

Finally, Figure 7 compares the steady-state and the transient-long-time rates, k_{ss} and k_{LT}, plotted as a function of N, for model A, model B, and the modified model B defined above. k_{LT} is obtained by solving the dynamical eq 14 and fitting the long-time part of the time evolution of the donor population to an exponential function $\exp(-k_{LT}t)$. For the parameters chosen, the two rates are very similar; however, larger deviations are seen with the modified model B for larger N, as expected. Note that all of the results are practically identical in the tunneling regime, where the bridge is not physically occupied. It is also interesting to note that, for the modified model B, k_{ss} appears to be dominated by the upper bridge levels, whereas k_{LT} is very close to the rate associated with the unmodified B model ($\Gamma_B = 0$).

To end this section, we comment on the observed N

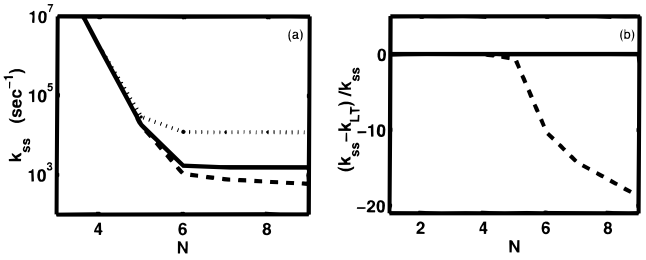

Figure 7. k_{ss} and k_{LT} plotted against the bridge length N. (a) Solid line: model A. Both k_{ss} and k_{LT} fall on the same line within the numerical resolution of this figure. Dotted line: model B. Again, k_{ss} and k_{LT} fall on the same line. Dashed line: k_{ss} in model B modified by adding damping terms $\Gamma_B = 2$ cm^{-1} to the dynamics of the lower bridge levels. This line lies almost on top of the lines that correspond to model A. In contrast, the results for k_{LT} in the modified B model (not shown) lie on top of those obtained for the unmodified B model. (b). The quantity $(k_{ss} - k_{LT})/k_{ss}$ plotted against N. The results for models A and B (solid line) are indistinguishable on this plot. Dashed line represents the results for the modified model B.

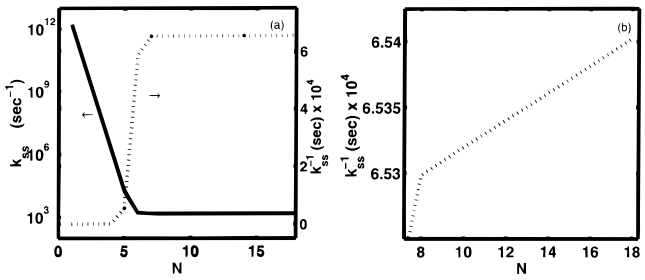

Figure 8. (a) k_{ss} and k_{ss}^{-1} plotted as functions of N. Solid line (left axis): k_{ss}. Dotted line (right axis): k_{ss}^{-1}. (b) k_{ss}^{-1} vs N shown above the crossover value of N on an expanded scale.

dependence of the transfer rate. As discussed above, the sequential hopping process that dominates the electron-transfer process above the crossover value of N appears to be practically independent of N. This seems, at first sight, contradictory to expectation, as this mode of transfer is usually associated with "Ohmic behavior", $k \sim N^{-1}$. We have recently[61] explained this behavior by noting that, above the crossover region, the steady-state rate satisfies

$$k_{ss}^{-1} = k_{up}^{-1} + k_{diff}^{-1} N \tag{29}$$

where k_{up} is the rate of population of the bridge and k_{diff} is the rate associated with diffusion through the bridge (see Figure 8). In the Markovian limit, where all relaxation rates are equal to κ, we have suggested the following approximate expressions:

$$k_{up} \sim \frac{V^2}{\Delta E^2} \kappa e^{-\Delta E/k_B T} \tag{30}$$

and

$$k_{diff} \sim \frac{4V^2}{\kappa} e^{-\Delta E/k_B T} \tag{31}$$

These expressions yield, with the parameters chosen for model A, $k_{up} \cong 1.1 \times 10^5$ s^{-1} and $k_{diff} = 3.8 \times 10^8$ s^{-1}. A numerical fit of results obtained for a model that is identical to model A but with $\tau_c = 0$ in eq 29 gives $k_{up} \cong 1.7 \times 10^5$ s^{-1} and $k_{diff} = 5.4 \times 10^8$ s^{-1}, in reasonable agreement with the theoretical estimates. Note that the non-Markovian case considered above is more complicated because the occurrence of several energy spacings in the diagonalized molecular Hamiltonian implies the existence of several relaxation rates. The qualitative behavior is, however, the same: The very weak N dependence seen above some crossover bridge length in Figures 2 and 3 is a manifestation of the existence of a range of N for which the electron transfer is dominated by the rate for thermally occupying the bridge. Such a range exists provided that $k_{up} < k_{diff}$, which, in the Markovian case, implies that $\Delta E > \kappa$ (cf. eqs 30 and 31).

TABLE 1: Bridge-length Dependence of the Transmission Rate

physical process	bridge-length (N) dependence	
super exchange (*small N, large* $\Delta E/V$, *large* $\Delta E/k_BT$)	$e^{-\beta N}$	$\beta = 2 \ln(V/\Delta E)$
steady-state hopping (*large N, small* $\Delta E/V$, *small* $\Delta E/k_BT$)	N^{-1}	
nondirectional hopping (*large N, small* $\Delta E/V$, *small* $\Delta E/k_BT$)	N^{-2}	
intermediate range (*intermediate N, small* $\Delta E/V$)	$(k_{up}^{-1} + k_{diff}^{-1} N)^{-1}$	$k_{up} \sim (V^2\kappa/\Delta E^2) e^{-\Delta E/k_B T}$ $k_{diff} \sim (4V^2/\kappa) e^{-\Delta E/k_B T}$ (Markovian case)
steady-state hopping + competing loss at every bridge site	$e^{-\alpha N}$	$\alpha = \sqrt{\Gamma_B(\Gamma_B + \kappa)}/2V$ (Markovian case)

In all cases, when $N \rightarrow \infty$, we find $k_{ss} \sim N^{-1}$. This result should be contrasted with the mean first passage time for unbiased diffusion. In that case, the mean time for a diffusing particle starting at one end of a 1-dimensional path to reach, for the first time, the other end scales like N^2.[49,68] The mean first passage time is, therefore, not a good measure for the steady-state rate and the associated conduction, but it may represent the intermediate-time behavior in transient experiments.

To summarize the results of the above discussion, Table 1 shows the different cases encountered in bridge-mediated electron transfer and the expected N dependence associated with each of them.

The experimentally observed N dependence is exponential, corresponding to the coherent tunneling mechanism described by eq 1, in many systems with sufficiently short N and sufficiently large ΔE. As N increases, the overall rate constant is expected to be a sum of coherent and incoherent contributions.[47] Incoherent tranfer dominates because the coherent contribution decays exponentially with N. The length dependence of the incoherent process can be quite complicated (Table 1), depending on the nature of the measurement and the effects of other parameters in both the system Hamiltonian and the bath environment. We emphasize again that, also in this limit, the rate may depend exponentially on N if other channels compete for the electron on the bridge.[67]

One simple electron-transfer system for which the two different limits have been observed is the phenylenevinylene-bridged tetracene/imide system of ref 48. At very short lengths this system behaves coherently, because the gap energy substantially exceeds the thermal energy, and nuclear tunneling is important; the decay with distance is then quite rapid, as suggested by eq 1. As the bridge becomes longer, the gap becomes smaller (both because of site interactions and because of etheric functionalization of the bridge), and when the gap becomes small enough ($N = 3$), activated transfer can occur. The case with the longer bridge exhibits only very weak length dependence. Although this experimental system does, indeed, show the transition from coherent superexchange to incoherent

hopping behavior, oversimplification can be dangerous: the temperature dependence of the motion in these systems exhibits gating-type behavior, as a result of internal rotations around the π-bonds in the bridge and the breakdown of the Condon approximation. The transition from coherent to incoherent behavior that accompanies changes in length and temperature is probably better illustrated in excitonic systems than in true electron-transfer structures.

6. Relation to Conductance

In section 4, we focused on a steady-state formulation of the electron-transfer rate problem, and we saw that, under certain conditions, the computed k_{ss} provides a good estimate of the rate associated with the long-time tail of the transfer process following a sudden excitation. Alternatively, steady-state experiments can be carried out, usually yielding current vs imposed electrostatic voltage data. In this section, we comment on the relationship between the k_{ss} associated with a given molecular bridge and the conductance of a junction based on the same molecule. In the latter case, the "donor" and "acceptor" levels ($|D\rangle$ and $|A\rangle$ in Figure 1) should be thought of as the Fermi energies for the metal junctions on the two sides of the molecular bridge. The well-known Landauer formula[62] provides a relation between the transmission coefficient T for a free particle that enters the junction from the left, say, to emerge on the right and the junction conductance[†78] g

$$g = \frac{e^2}{\pi\hbar} T(E_F) \tag{32}$$

where E_F is the Fermi energy of the metal junction at zero voltage bias. This result was derived under the assumption that possible dephasing processes involve only quasi-elastic scattering, that is, they involve no energy relaxation. We have recently shown[61] that this result can be generalized, under fairly general conditions, to situations involving activated transport, such as encountered in the present work. Focusing on a form equivalent to eq 32

$$g = e^2 k'_{ss}(E_F)\rho_i(E_F) \tag{33}$$

where ρ_i is the density of states in the initial metal manifold and $k'_{ss}(E_F)$ is the steady-state transfer rate associated with an initial metal state at the Fermi energy, we have found that this form remains valid in the presence of activated transmission via the bridge, except that k'_{ss} becomes the total (elastic and inelastic) transmission rate. It should be emphasized that this rate is different from a "standard" electron-transfer rate, k_{ss}. Apart from differences associated with details of the electronic structure of specific systems, there is one important general aspect: The former rate involves a delocalized metal state, whereas the latter is the transfer rate associated with an initial state localized on a donor molecule. The difference enters in the relationship between the matrix elements connecting these initial states to the neighboring bridge state: Their ratio should scale like $(l_M/L)^{1/2}$, where L is the size of the (1-dimensional) metal and l_M is the characteristic size of the donor state, typically the size of a molecular site. Consequently,

$$k'_{ss} = k_{ss}\frac{l_M}{L} \tag{34}$$

Using also

$$\rho_i(E_F) = \frac{L}{2\pi\hbar}\sqrt{\frac{2m}{E_F}} \tag{35}$$

where m is the electron mass, we obtain

$$g = \frac{e^2}{\pi\hbar} l_M k_{ss}\sqrt{\frac{m}{2E_F}} \tag{36}$$

A comparison of eq 36 to eq 32 yields a definition for an effective transmission coefficient

$$T_{eff} = l_M k_{ss}\sqrt{\frac{m}{2E_F}} \tag{37}$$

Using, for example, $E_F = 3$ eV and $l_M = 5$ Å leads to

$$T_{eff} \sim (2.5 \times 10^{-16}) \times k_{ss}\,(s^{-1}) \tag{38}$$

and

$$g\,(\Omega^{-1}) \sim 10^{-20} \times k_{ss}\,(s^{-1}) \tag{39}$$

With a current detector sensitive to picoamperes, k_{ss} must exceed 10^8 s^{-1} before measurable current can be observed at a 1-V voltage across such a junction.

7. Coherent vs Incoherent Transfer

How can we decide whether an observed electron-transfer process proceeds by coherent tunneling or by sequential hopping? In the experiment of ref 48, which uses poly(*p*-phenylenevinylene) chains of varying length as bridges between organic donors and acceptors, the fast decrease of the electron-transfer rate with bridge length for 1−2 bridge units, followed by weak dependence on length for 3−5 bridge units, can be interpreted as a transition from tunneling to hopping, as seen in Figures 2 and 3. However, this interpretation cannot be made unequivocally, because the energy gap ΔE between the donor/acceptor and the bridge in these compounds decreases with increasing bridge length. For a given positive value of ΔE, we expect that temperature-independent coherent tunneling at very low temperatures will become thermally activated hopping transport at some higher temperature, as seen in Figure 6. This behavior has been observed in certain bridge-mediated electron-transfer processes, such as the chemically modified B-vinyl(A) reaction center;[69] however, it has not yet been seen in molecular wires. Note that, if ΔE is very small or negative (that is, if the donor level is close to or higher than the ground vibronic bridge level), the hopping route is also activationless, and thermal activation will not be seen. Furthermore, when the donor level is substantially higher than the ground bridge energy, incoherent sequential hopping may result from the irregular nature of the coupling between states belonging to vibronic manifolds on neighboring bridge sites, even without thermal dephasing.[49]

An interesting way to distinguish between the coherent tunneling and sequential hopping modes of electron transfer has been suggested by Grozema et al.[70] in their analysis of electron transfer in donor−DNA−acceptor systems. These authors have pointed out that, for a bridge of adenine−thymine (AT) base pairs, the exchange of an AT base pair by a guanine−cytosine (GC) base pair, which corresponds to a lower energy of this "impurity" bridge site, increases the electron-transfer rate.[67a] They argue that this observation agrees with a prediction based on coherent tunneling and stands in contrast to expectations based on the sequential hopping model. We note that the validity

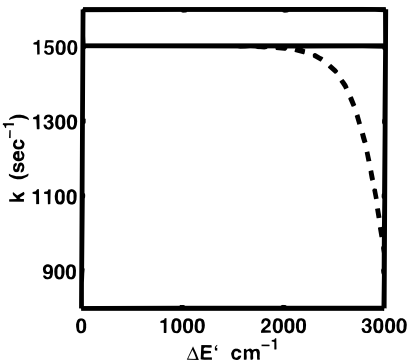

Figure 9. Rates associated with model A′ (see text) in the classical limit, as functions of $\Delta E'$. Solid line: k_{ss}. Dashed line: k_{LT}.

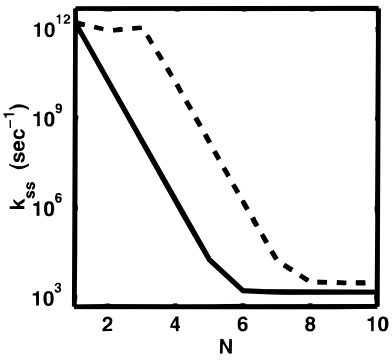

Figure 10. Steady-state rate, k_{ss}, plotted against the bridge length N for the quantum models A (solid line) and A′ (dashed line).

of the time-dependent self-consistent field approach used in the calculation of the coupled vibrational−electronic motion in the model used in ref 70 is questionable.[71] We show below that, although our model reproduces some of the qualitative aspects of that study, the overall effect of substituting an impurity site on the bridge is considerably more involved.

Consider first the completely classical model, where the transfer proceeds by a hopping between levels according to

$$\frac{dP_n}{dt} = -(k_{n-1\leftarrow n} + k_{n+1\leftarrow n})P_n + k_{n\leftarrow n-1}P_{n-1} + k_{n\leftarrow n+1}P_{n+1} \quad (40)$$

where P_n is the population at site n and where

$$k_{n\leftarrow m} = \begin{cases} k_0 \exp\left(-\dfrac{E_n - E_m}{k_B T}\right) & E_n > E_m \\ k_0 & \text{otherwise} \end{cases} \quad (41)$$

Using this kinetic scheme, we compare the rates associated with the energy levels defined by model A (section 5) and by a model (denoted A′) that is derived from model A by lowering the energy of the site $n = 2$ by $\Delta E'$. An important observation is that, for this model, the steady-state rate, k_{ss}, does not depend on $\Delta E'$ (see Appendix C). We obtain, for this case,

$$k_{ss} = \frac{\Gamma_A k_0 e^{-\Delta E/k_B T}}{k_0 e^{-\Delta E/k_B T} + (N+1)\Gamma_A} \quad (42)$$

In contrast, the rate k_{LT}, which is derived from the long-time tail of the donor survival probability, does depend on $\Delta E'$. In particular, for the original model A ($\Delta E' = 0$), k_{LT} is very close to k_{ss}; however, k_{LT} decreases with increasing $\Delta E'$, as noted in ref 70. This is seen in Figure 9, which displays k_{ss} and k_{LT} as functions of $\Delta E'$.

Next, consider the time evolution described by the quantum scheme used in sections 2−5. In the following calculations, we take $\Delta E' = \Delta E$, so that $E_D = E_A = E_2$, whereas the values of $E_n - E_D$, $n = 1, 3, 4, ..., N$, remain constant at 3000 cm^{-1}, as before. Figure 10 shows the steady-state rate as a function of bridge length N, as computed for models A and A′. Obviously, the rate in the superexchange regime of model A′ is considerably larger than the corresponding rate in model A. Perhaps surprisingly, rates observed for N beyond the crossover region also show the same trend, specifically, $k_{ss}^{(A)} < k_{ss}^{(A')}$, unlike the result that could be inferred from ref 70. We recall that, for the intermediate range of N shown here, the steady-state rate in the hopping regime is dominated by the rate for populating the bridge, not by that for hopping through the bridge, and this rate becomes higher when one bridge level (and, therefore, the band of diagonalized molecular states) is lowered. We expect that, for much longer bridges, for which the overall rate is determined by the classical hopping dynamics, the trend will reflect the observation made in the classical limit.

We conclude that the effect of inserting an impurity site into the bridge can, indeed, distinguish between coherent tunneling and incoherent transfer; however, this distinction depends on the mode (such as transient or steady-state) of the experiment and on details of the measurement. It should be noted that the above analysis cannot be applied to the model[49] in which incoherent hopping is associated with irregular vibronic coupling between bridge sites in a system with $E_D > E_{bridge}$. In this model, the effect of lowering the electronic origin of one bridge site on the overall transfer rate depends on details of the energy-dependent density of states and the Franck−Condon factors that control coupling between bridge sites.

We end this discussion by noting that there is, in principle, one more way to distinguish between coherent and incoherent modes of electron transfer. If we could devise a system with two pathways (for example, two molecular bridges) connecting the donor and the acceptor, coherent transfer should show interference between these routes, whereas the single pathway rates will combine additively in the incoherent case. To test this idea, a system constructed for this purpose should have the capability of switching off any one pathway in order to study the way in which the pathways combine.

8. Concluding Remarks

Transfer of charge from an initial, localized donor state to a final, localized acceptor state through a structured linking bridge is a very common motif in synthetic and biological molecular structures. Extensive experimental and theoretical analysis has been devoted to this problem, often in the limit where the excitation gap between the donor states and the bridge states is so large that only coherent tunneling processes (in which the bridge is never actually occupied) can contribute to the rate process.

Several recent studies, experimental and theoretical, have considered the situation in which occupation of the bridge levels can occur and, therefore, incoherent processes can be seen. Our current analysis considers various aspects of this rich and important problem. We observe several different regimes of distance dependence, ranging from fairly rapid exponential decrease in the coherent superexchange regime to an inverse length dependence in the incoherent diffusive limit (or very weak exponential decay in the case of a "leaky" bridge) to a nearly distance-independent behavior in the intermediate regime. The variations among these regimes depend intimately on the role

of the environment in acting as a sink and source of energy and as a dephasing medium.[72] In addition to the distance dependence, different regimes of temperature dependence are observed: tunneling transport occurs at low temperatures and activated passage over barriers takes place at higher temperatures.

Thus, we expect different modes of behavior depending on the energetics, the temperature, the bridge length, the strength of the system−bath interactions, and the existence of competing channels. Furthermore, different results may be obtained for steady-state and transient situations.

Recent experiments on DNA, the photosynthetic reaction center, proteins, and synthetic donor−bridge−acceptor systems indicate explicitly that these different regimes of charge transport have indeed been observed. The current analysis presents energy criteria for the observation of the different regimes, as well as the corresponding distance and temperature dependencies.

The analogy between conductance measurements in molecular circuits and rate measurements in donor−bridge−acceptor compounds suggests that the Landauer formula can be extended not only to deal with coherent and elastic dephasing situations but also to characterize activated transport in molecular circuitry. This conductivity/rate correspondence suggests that several experimental means exist that can distinguish between coherent and incoherent modes of charge transfer. These include substitution of impurities on the bridge, examination of interference between two bridge pathways, and careful measurement of the temperature dependence of the transmission rate or yield.

Acknowledgment. This research was supported in part by the USA−Israel Binational Science Foundation (A.N.) and the Chemistry Divisions of the DOE, the NSF, and the ONR and also by the DOD/MURI program (M.A.R.). D.S. and A.N. thank Philipp Maass, David Tannor, and Eitan Geva for helpful discussions.

Appendix A

In the discussion that follows, we denote by $\{n\}$ the local basis (eigenstates of H_0) and by $\{\nu\}$ the basis of molecular eigenstates (eigenstates of $H_M = H_0 + V$). The Hamiltonian can be written generally as

$$H = H_B + \sum_n E_n^0 |n\rangle\langle n| + \sum_{n\neq n'}\sum V_{nn'}|n\rangle\langle n'| + \sum_{nn'}\sum F_{nn'}|n\rangle\langle n'| \quad \text{(A1)}$$

or

$$H = H_B + \sum_\nu E_\nu |\nu\rangle\langle\nu| + \sum_\nu\sum_{\nu'} \bar{F}_{\nu\nu'}|\nu\rangle\langle\nu'| \quad \text{(A2)}$$

The reduced equation of motion for the molecular density matrix is written in these two representations as follows:

$$\dot{\sigma}_{nn'} = -i\omega^0_{nn'}\sigma_{nn'} - i[V,\sigma]_{nn'} + \sum_{n_1n_2}\sum R_{nn'n_1n_2}\sigma_{n_1n_2} \quad \text{(A3)}$$

and

$$\dot{\sigma}_{\nu\nu'} = -i\omega_{\nu\nu'}\sigma_{\nu\nu'} + \sum_{\nu_1\nu_2}\sum \bar{R}_{\nu\nu'\nu_1\nu_2}\sigma_{\nu_1\nu_2} \quad \text{(A4)}$$

Let T be the unitary transformation from the molecular to the local basis.

$$|n\rangle = \sum_\nu T_{n\nu}|\nu\rangle;\ T^+ = T^{-1} \quad \text{(A5)}$$

Then

$$\bar{F}_{\nu\nu'} = \sum_n\sum_{n'} T_{n\nu}T^*_{n'\nu'}F_{nn'} \quad \text{(A6)}$$

$$F_{nn'} = \sum_\nu\sum_{\nu'} T^*_{n\nu}T_{n'\nu'}\bar{F}_{\nu\nu'} \quad \text{(A7)}$$

$$\bar{R}_{\nu\nu'\nu_1\nu_2} = \sum_n\sum_{n'}\sum_{n_1}\sum_{n_2} T_{n\nu}T^*_{n_1\nu_1}T_{n_2\nu_2}T^*_{n'\nu'}R_{nn'n_1n_2} \quad \text{(A8)}$$

$$R_{nn'n_1n_2} = \sum_\nu\sum_{\nu'}\sum_{\nu_1}\sum_{\nu_2} T^*_{n\nu}T_{n_1\nu_1}T^*_{n_2\nu_2}T_{n'\nu'}\bar{R}_{\nu\nu'\nu_1\nu_2} \quad \text{(A9)}$$

are the prescriptions to transform between the two representations.

Appendix B

The problem of classical 1-dimensional hopping with a constant loss term at each site is represented by the following master equation (see also ref 68):

$$\dot{P}_n = -(2k_B + \Gamma_B)P_n + k_B(P_{n+1} + P_{n-1});\ 0 < n < N$$
$$\dot{P}_N = -(k_B + \Gamma_A + \Gamma_B)P_N + k_BP_{N-1};\ n = N \quad \text{(B1)}$$

where k_B is the hopping rate between bridge sites, Γ_B (assumed to be much smaller than k_B) is the loss rate at each site, and Γ_A is the escape rate at the last site N. At steady state, the flux balance at site n is $k_B(P_{n-1} - P_n) - k_B(P_n - P_{n+1}) = \Gamma_BP_n$, or

$$k_B(P_{n-1} + P_{n+1} - 2P_n) = \Gamma_BP_n \quad \text{(B2)}$$

Looking for a solution of the form $P_n = x^n$, we find, to lowest order in Γ_B/k_B,

$$x = 1 \pm \sqrt{\Gamma_B/k_B} \quad \text{(B3)}$$

An approximate form for the solution that satisfies $P_0 = 1$ is

$$P_n = A\exp[-\sqrt{\Gamma_B/k_B}\,n] + (1 - A)\exp[\sqrt{\Gamma_B/k_B}\,n] \quad \text{(B4)}$$

and A can be determined by the other boundary condition, which is the steady-state version of the second line of eq B1, $P_N = k_B(k_B + \Gamma_A + \Gamma_B)^{-1}P_{N-1}$. The (intuitively obvious) result is $A \cong 1$, so the N dependence of the transmitted flux, $J(N) = \Gamma_AP_N$, is

$$J(N) \sim \exp(-\sqrt{\Gamma_B/k_B}\,N) \quad \text{(B5)}$$

Consider now the equivalent quantum mechanical problem: A quantum particle moves on a 1-dimensional lattice, with all site energies equal and with nearest-neighbor coupling V. The amplitude at site n satisfies

$$\dot{C}_n = -iV(C_{n-1} + C_{n+1}) - (1/2)\Gamma_BC_n;\ n \neq 0, N$$
$$\dot{C}_N = -iVC_{N-1} - (1/2)(\Gamma_B + \Gamma_A)C_N \quad \text{(B6)}$$

Solving for a steady state with $C_0 = 1$ leads, for large N, to

$$J = \Gamma_A|C_N|^2 \sim e^{-(\Gamma_B/2V)N} \quad \text{(B7)}$$

We note in passing that a comparison of eqs B7 and B5 leads to an effective hopping rate for the quantum case

$$k_B = 4V^2/\Gamma_B \tag{B8}$$

which is the same form as eq 31, although Γ_B replaces κ as the characteristic relaxation time. When both damping and dephasing occur on the bridge, we expect

$$k_B = 4V^2/(\Gamma_B + \kappa) \tag{B9}$$

and using this expression in eq B5 yields

$$J(N) \sim e^{-[\sqrt{\Gamma_B(\Gamma_B + \kappa)}/2V]N} \tag{B10}$$

We have verified numerically that, for large N, the same result holds also when $\Delta E \neq 0$.

Appendix C

Consider the following classical kinetic scheme for electron migration in a nearest-neighbor coupling model:

$$\begin{aligned}
\dot{P}_0 &= -k_{10}P_0 + k_{01}P_1 \\
\dot{P}_1 &= -(k_{01} + k_{21})P_1 + k_{10}P_0 + k_{12}P_2 \\
\dot{P}_2 &= -(k_{12} + k_{32})P_2 + k_{21}P_1 + k_{23}P_3 \\
&\vdots \\
\dot{P}_N &= -(k_{N-1,N} + k_{N+1,N})P_N + k_{N,N-1}P_{N-1} + k_{N,N+1}P_{N+1} \\
\dot{P}_{N+1} &= -k_{N,N+1}P_{N+1} + k_{N+1,N}P_N - \Gamma_A P_{N+1}
\end{aligned} \tag{C1}$$

where $P_k = \sigma_{kk}$ is the polupation in level k. In our models A and A′,

$$\begin{aligned}
k_{10} &= k_{N,(N+1)} = k_0 e^{-\Delta E/k_B T} \\
k_{n-1,n} &= k_{n+1,n} = k_0 e^{-\Delta E'/k_B T} \ (n\text{-impurity level})
\end{aligned} \tag{C2}$$

and all other rates equal k_0. We consider a steady state imposed by setting $P_0 = 1$ and disregarding the equation for $\dot{P}_0$ in eq C1. Summing all of the other steady-state equations yields

$$0 = k_{10}P_0 - k_{01}P_1 - \Gamma_A P_{N+1} \tag{C3}$$

whereas summing the last $N - n + 1$ equations ($n = 1, 2, ..., N$) leads to

$$0 = k_{n+1,n}P_n - k_{n,n+1}P_{n+1} - \Gamma_A P_{N+1} \tag{C4}$$

Summing all of the $N + 1$ equations generated by eqs C3 and C4, using the fact that $k_{n-1,n} = k_{n+1,n}$ for all $n \neq 0$, $N + 1$, leads to

$$0 = k_{10}P_0 - k_{N,N+1}P_{N+1} - (N+1)\Gamma_A P_{N+1} \tag{C5}$$

whence

$$P_{N+1} = k_{10}P_0/[k_{N,N+1} + (N+1)\Gamma_A] \tag{C6}$$

and

$$k_{ss} = \Gamma_A P_{N+1}/P_0 = k_{10}\Gamma_A/[k_{N,N+1} + (N+1)\Gamma_A] \tag{C7}$$

Using eq C2 in eq C7 then yields eq 42.

References and Notes

(1) Marcus, R. A. *Rev. Mod. Phys*. **1993**, *65*, 599. Kuznetsov, A. M. *Charge Transfer in Physics, Chemistry and Biology*; Gordon & Breach: New York, 1995.

(2) Bixon, M.; Jortner, J. *Adv. Chem. Phys*. **1999**, *106*, 35.

(3) Newton, M. D. *Chem. Rev*. **1991**, *91*, 767. Billing, G. D.; Mikkelsen, K. V. *Molecular Dynamics and Chemical Kinetics*; Wiley: New York, 1996.

(4) Barbara, P. F.; Meyer, T. J.; Ratner, M. A. *J. Phys. Chem*. **1996**, *100*, 13148.

(5) Marcus, R. A.; Sutin, N. *Biochim. Biophys. Acta* **1985**, *811*, 265.

(6) Wasielewski, M. R. *Chem. Rev*. **1992**, *92*, 435.

(7) Wasielewski, M. R.; Niemczyk, M. P.; Johnson, D. G.; Svec, W. A.; Minsek, D. W. *Tetrahedron* **1989**, *45*, 4785.

(8) Magoga, M.; Joachim, C. *Phys. Rev. B: Condens. Matter Mater. Phys*. **1998**, *57*, 1820−1823. Joachim, C.; Vinuesa, J. F. *Eur. Phys. Lett*. **1996**, *33*, 635.

(9) Sachs, S. B.; Dudek, S. P.; Sita, L. R.; Smalley, J. F.; Newton, M. D.; Feldberg, S. W.; Chidsey, C. E. D. *J. Am. Chem. Soc*. **1997**, *119*, 10563.

(10) Grosshenny, V.; Harriman, A.; Ziessel, R. *Angew. Chem., Int. Ed. Engl*. **1996**, *34*, 2705.

(11) Tour, J. M. *Chem. Rev*. **1996**, *96*, 537.

(12) Osuka, A.; Tanabe, N.; Kawabata, S.; Yamazaki, I.; Nishimura, Y. *J. Org. Chem*. **1995**, *60*, 7177.

(13) (a) Ribou, A.-C.; Launay, J.-P.; Takahashi, K.; Nihira, T.; Tarutani, S.; Spangler, C. W. *Inorg. Chem*. **1994**, *33*, 1325. (b) Woitellier, S.; Launay, J. P.; Spangler, C. W. *Inorg. Chem*. **1989**, *28*, 758.

(14) Helms, A.; Heiler, D.; McLendon, G. *J. Am. Chem. Soc*. **1992**, *114*, 6227.

(15) Tolbert, L. M. *Acc. Chem. Res*. **1992**, *25*, 561.

(16) Arrhenius, T. S.; Blanchard-Desce, M.; Dvolaitzky, M.; Lehn, J.-M.; Malthete, J. *Proc. Natl. Acad. Sci. U.S.A*. **1986**, *83*, 5355.

(17) Finkh, P.; Heitele, H.; Volk, M.; Michel-Beyerle, M. E. *J. Phys. Chem*. **1988**, *92*, 6584−6590.

(18) Ziessel, R. F. *J. Chem. Educ*. **1997**, *74*, 673−679.

(19) (a) Bjerrrum, M. J.; Casimiro, D. R.; Chang, I.-J.; DiBilio, A. J.; Gray, H. B.; Hill, M. G.; Langen, R.; Mines, G. A.; Skov, L. K.; Winkler, J. R.; Wuttke, D. S. *J. Bioenerg. Biomembr*. **1995**, *27*, 295. (b) Langen, R.; Chang, I.-J.; Germanas, J. P.; Richards, H. J.; Winkler, J. R.; Gray, H. B. *Science* **1995**, *268*, 1733. (c) Winkler, J. R.; Gray, H. B. *Chem. Rev*. **1992**, *92*, 381.

(20) Ogawa, M. Y.; Wishart, J. F.; Young, Z.; Miller, J. R.; Isied, S. S. *J. Phys. Chem*. **1993**, *97*, 11456. Isied, S. S.; Ogawa, M. Y.; Wishart, J. F. *Chem. Rev*. **1992**, *92*, 381.

(21) Schanze, K. S.; Cabana, L. A. *J. Phys. Chem*. **1990**, *94*, 2740.

(22) Vanderkooi, J. M.; Englander, S. W.; Papp, S.; Wright, W. W. *Proc. Natl. Acad. Sci. U.S.A*. **1990**, *87*, 5099.

(23) Moser, C. E.; Page, C. C.; Farid, R.; Dutton, P. L. *J. Bioenerg. Biomembr*. **1995**, *27*, 263−274.

(24) Mutz, M. W.; Case, M. A.; Wishart, J. F.; Ghadiri, M. R.; McLendon, G. L. *J. Am. Chem. Soc*. **1999**, *121*, 858−859.

(25) Lewis, F. D.; Wu, T.; Zhang, Y.; Letsinger, R. L.; Greenfield, S. R.; Wasielewski, M. R. *Science* **1997**, *277*, 673.

(26) Holmlin, R. E.; Dandliker, P. J.; Barton, J. K. *Angew. Chem., Int. Ed. Engl*. **1997**, *36*, 2714.

(27) Lincoln, P.; Tuite, E.; Norden, B. *J. Am. Chem. Soc*. **1997**, *119*, 1454.

(28) Brun, A. M.; Harriman, A. *J. Am. Chem. Soc*. **1994**, *116*, 10383.

(29) Meade, T. J.; Kayyem, J. F. *Angew. Chem., Int. Ed. Engl*. **1995**, *34*, 352−354.

(30) Barbara, P. F.; Olson, E. J. C. *Adv. Chem. Phys*. **1999**, *107*, 647−676.

(31) Fukui, K.; Tanaka, K. *Angew. Chem., Int. Ed. Engl*. **1998**, *37*, 158−161.

(32) Meggers, E.; Kusch, D.; Spichty, M.; Wille, U.; Giese, B. *Angew. Chem., Int. Ed. Engl*. **1998**, *37*, 460−462.

(33) Ghiggino, K. P.; Clayton, A. H. A.; Lawson, J. M.; Paddon-Row, M. N. *New J. Chem*. **1996**, *20*, 853. Oevering, H.; Paddon-Row, M. N.; Heppener, M.; Oliver, A. M.; Cotsaris, E.; Verhoeven, J. W.; Hush, N. S. *J. Am. Chem. Soc*. **1987**, *109*, 3258.

(34) Carter, M. T.; Rowe, G. K.; Richardson, J. N.; Tender, L. M.; Terrill, R. H.; Murray, R. W. *J. Am. Chem. Soc*. **1995**, *117*, 2896.

(35) Guo, L.-H.; Facci, J. S.; McLendon, G. *J. Phys. Chem*. **1995**, *99*, 8458.

(36) Paulson, B.; Pramod, K.; Eaton, P.; Closs, G.; Miller, J. R. *J. Phys. Chem*. **1993**, *97*, 13042. Johnson, M. D.; Miller, J. R.; Green, N. S.; Closs, G. L. *J. Phys. Chem*. **1989**, *93*, 1173.

(37) Stein, C. A.; Lewis, N. A.; Seitz, G. *J. Am. Chem. Soc*. **1982**, *104*, 2596.

(38) Evenson, J. W.; Karplus, M. *J. Chem. Phys.* **1992**, *96*, 5272; *Science* **1993**, *262*, 1247. Hsu, C. P.; Marcus, R. A. *J. Chem. Phys.* **1997**, *106*, 504.
(39) Meade, T. J. In *Metal Ions in Biological Systems*; Sigel, A., Sigel, H., Eds.; Marcel Dekker, Inc.: New York, 1996; Vol. 33, p 453.
(40) Miller, J. R.; Beitz, J. V. *J. Chem. Phys.* **1981**, *74*, 6746.
(41) Beratan, D. N.; Betts, J.; Onuchic, J. N. *Science* **1991**, *252*, 1285. Stuchebrukhov, A. A. *J. Chem. Phys.* **1996**, *104*, 8424.
(42) McConnell, H. M. *J. Chem. Phys.* **1961**, *35*, 508.
(43) Goldman, C. *Phys. Rev. A* **1991**, *43*, 4500.
(44) Ratner, M. A. *J. Phys. Chem.* **1990**, *94*, 4877.
(45) Won, Y.; Friesner, R. A. *Biochim. Biophys. Acta* **1988**, *935*, 9−18.
(46) Hsu, C.-P.; Marcus, R. A. *J. Chem. Phys.* **1997**, *106*, 584−598.
(47) Davis, W. B.; Wasielewski, M. R.; Ratner, M. A.; Mujica, V.; Nitzan, A. *J. Phys. Chem. A* **1997**, *101*, 6158−6164.
(48) Davis, W. B.; Svec, W. A.; Ratner, M. A.; Wasielewski, M. R. *Nature* **1998**, *396*, 60−63.
(49) Jortner, J.; Bixon, M.; Langenbacher, T.; Michel-Beyerle, M. E. *Proc. Natl. Acad. Sci. U.S.A.* **1998**, *95*, 12759−12765.
(50) Reimers, J. R.; Hush, N. S. *Chem. Phys.* **1989**, *134*, 323; *J. Photochem. Photobiol.* **1994**, *A82*, 31.
(51) Medvedev, E. S.; Stuchebrukhov, A. A. *J. Chem. Phys.* **1997**, *107*, 3821.
(52) Felts, A. K.; Pollard, W. T.; Friesner, R. A. *J. Phys. Chem.* **1995**, *99*, 2929. Pollard, W. T.; Felts, A. K.; Friesner, R. A. *Adv. Chem. Phys.* **1996**, *93*, 77 and references therein.
(53) Redfield, A. G. *IBM J. Res. Dev.* **1957**, *1*, 19; *Appl. Magn. Reson.* **1965**, *1*, 1.
(54) Okada, A.; Chernyak, V.; Mukamel, S. *J. Phys. Chem. A* **1998**, *102*, 1241. Skourtis, S. S.; Mukamel, S. *Chem. Phys.* **1995**, *197*, 367−388.
(55) Makri, N.; Marakov, D. E. *J. Chem. Phys.* **1995**, *102*, 4600, 4611.
(56) Meier, C.; Tannor, D. J. *Non-Markovian Evolution of the Density Operator in the Presence of Strong Laser Fields*, to be published.
(57) Tanimura, Y.; Wolynes, P. G. *Phys. Rev. A* **1991**, *43*, 4131; *J. Chem. Phys.* **1992**, *96*, 8485.
(58) Bartana, A.; Kosloff, R.; Tannor, D. J. *J. Chem. Phys.* **1997**, *106*, 1435 and references therein.
(59) Büttiker, M. *IBM J. Res. Dev.* **1988**, *32*, 63.
(60) Imry, Y. *Introduction to Mesoscopic Physics*; Oxford University Press: New York, 1997; Chapter 3 and references therein.
(61) Segal, D.; Nitzan, A.; Ratner, M.; Davis, W. D. To be published.
(62) Landauer, R. *IBM J. Res. Dev.* **1957**, *1*, 223. See also ref 60.
(63) Slichter, C. P. *Principles of Magnetic Resonance*; Springer: New York, 1990. Schatz, G. C.; Ratner, M. A. *Quantum Mechanics in Chemistry*; Prentice Hall: New York, 1993. Mukamel, S. *Principles of Nonlinear Optical Spectroscopy*; Oxford University Press: Oxford, 1995.
(64) It should be emphasized that the original derivation of the Redfield equations[53] was done using a representation in which H_M is diagonal, that is, $V = 0$. This is the way the Redfield equations are used in ref 52 and in most of the magnetic resonance literature, but not in the quantum optics literature.
(65) Harris, R. A.; Silbey, R. *J. Chem. Phys.* **1985**, *83*, 1069.
(66) Kramers, H. A. *Physica (Utrecht)* **1940**, *7*, 284. For recent reviews and applications, see: Fleming, G. R., Hänggi, P., Eds. *Activated Barrier Crossing*; World Scientific: Singapore, 1993.
(67) (a) Meggers, E.; Michel-Beyerle, M. E.; Giese, B. *J. Am. Chem. Soc.* **1998**, *120*, 12950−12955. (b) Giese, B.; Wessely, S.; Spormann, M.; Lindemann, U.; Meggers, E.; Michel-Beyerle, M. E. *Angew. Chem., Intl. Ed.* **1999**, *38*, 996−998. (c) Henderson, P. T.; Jones, D.; Hampikian, G.; Kan, Y.; Schuster, G. B. *Proc. Natl. Acad. Sci. U.S.A.* **1999**, *96*, 8353. (d) Wan, C.; Fiebig, T.; Kelly, S. O.; Treadway, C. R.; Barton, J. K.; Zewail, A. H. *Proc. Natl. Acad. Sci. U.S.A.* **1999**, *86*, 6014. (e) Bixon, M.; Giese, B.; Wessely, S.; Langenbacher, T.; Michel-Beyerle, M. E.; Jortner, J. *Proc. Natl. Acad. Sci. U.S.A.* To be published.
(68) Landauer, R.; Buttiker, M. *Phys. Rev. B* **1987**, *36*, 6255.
(69) Hartwich, G.; Bieser, G.; Langenbacher, T.; Müller, P.; Richter, M.; Ogrodnik, A.; Scheer, H.; Michel-Beyerle, M. E. *Biophys. J.* **1997**, *71*, A8.
(70) Grozema, F. C.; Berlin, Y. A.; Siebbeles, L. D. A. *Int. J. Quant. Chem.* In press.
(71) See, for example: Kotler, Z.; Neria, E; Nitzan, A. *Comput. Phys. Commun.* **1991**, *63*, 243 and references therein.
(72) In molecular crystals, the existence of coherent and incoherent energy-transfer regimes has long been recognized. See, for example: Silbey, R. *Annu. Rev. Phys. Chem.* **1976**, *27*, 203.
(73) For example, the application of eq 15 to the model

$$H = H_M + H_B + F_{11}|1\rangle\langle 1| + F_{22}|2\rangle\langle 2|$$

$$H_M = E_1|1\rangle\langle 1| + E_2|2\rangle\langle 2| + V_{12}|1\rangle\langle 2| + V_{21}|2\rangle\langle 1|$$

with bath operators that satisfy $\langle F_{11}(t)F_{22}(0)\rangle = 0$, leads to equations of the form

$$\dot{\sigma}_{11} = -\dot{\sigma}_{22} = -\mathrm{i}(V_{12}\sigma_{21} - V_{21}\sigma_{12})$$

$$\dot{\sigma}_{12} = \dot{\sigma}^*_{21} = -\mathrm{i}\omega_{12}\sigma_{12} - \mathrm{i}V_{12}(\sigma_{22} - \sigma_{11}) - 1/2\kappa\sigma_{12}$$

where $\omega_{12} = E_1 - E_2 + \Delta\omega$, and where κ and $\Delta\omega$ (both small relative to ω_{12}) are defined in terms of Fourier transforms of the time correlation functions involving F_{11} and F_{22}. The equilibrium ($t \rightarrow \infty$) solution of the last pair of equations is easily shown to be $\sigma_{11} = \sigma_{22} = 1/2$; $\sigma_{12} = \sigma_{21} = 0$, irrespective of the magnitudes of ω_{12} and V, *provided that* $V \neq 0$.
(74) Note that the continuous manifolds shown on the right and left in Figure 1 do not appear here explicitly. Instead, the width Γ_A imposed on the acceptor level represents the effect of the manifold on the right. An equivalent width Γ_D will be imposed on the donor (and a constant population σ_{AA} imposed on the acceptor) when the reverse flux is considered.
(75) Although the Gaussian form, $\exp[-(1/2\tau_c\omega)^2]$, in eq 28 is familiar in the literature, recent analysis of rate processes associated with large energy gaps (D. Rostkier-Edelstein, P. Graf, and A. Nitzan, *J. Chem. Phys.* **1997**, *107*, 10470 and references therein) show that an exponential energy gap law, $\exp(-\tau_c\omega)$, provides a better description. Our qualitative discussion does not depend on this observation.
(76) The parameter κ could be varied by changing the pressure in an experiment performed above the critical temperature of the solvent.
(77) †Note that Figure 4 shows results for a non-Markovian case. In the Markovian limit, $\tau_c = 0$, where all relaxation rates are equal to κ, we have verified numerically that the transition region may be estimated from the relation $\kappa \approx 2\Delta E N^{-1/2}$. This is the condition for a maximum in the flux, which is given approximately by $\kappa V^2[\Delta E^2 + (\kappa/2)^2 N]^{-1}\mathrm{e}^{-\Delta E/k_B T}$ (cf. eqs 29−31).
(78) †For a discussion of the difference between the result in eq 32 and the original formulation of ref 62, in which T is replaced by $T/(1 - T)$, see, for example, ref 60, chapter 5.